



CHORUS

This is the accepted manuscript made available via CHORUS. The article has been published as:

Statistical Transmutation in Floquet Driven Optical Lattices

Tigran A. Sedrakyan, Victor M. Galitski, and Alex Kamenev

Phys. Rev. Lett. **115**, 195301 — Published 4 November 2015

DOI: [10.1103/PhysRevLett.115.195301](https://doi.org/10.1103/PhysRevLett.115.195301)

Statistical transmutation in Floquet driven optical lattices

Tigran A. Sedrakyan,^{1,2} Victor M. Galitski,^{3,4} and Alex Kamenev¹

¹*William I. Fine Theoretical Physics Institute, University of Minnesota, Minneapolis, Minnesota 55455, USA*

²*Physics Frontier Center and Joint Quantum Institute,*

University of Maryland, College Park, Maryland 20742, USA

³*Joint Quantum Institute and Condensed Matter Theory Center, Department of Physics,*
University of Maryland, College Park, Maryland 20742-4111, USA

⁴*School of Physics, Monash University, Melbourne, Victoria 3800, Australia*

(Dated: October 16, 2015)

We show that interacting bosons in a periodically-driven two dimensional (2D) optical lattice may effectively exhibit fermionic statistics. The phenomenon is similar to the celebrated Tonks-Girardeau regime in 1D. The Floquet band of a driven lattice develops the moat shape, i.e. a minimum along a closed contour in the Brillouin zone. Such degeneracy of the kinetic energy favors fermionic quasiparticles. The statistical transmutation is achieved by the Chern-Simons flux attachment similar to the fractional quantum Hall case. We show that the velocity distribution of the released bosons is a sensitive probe of the fermionic nature of their stationary Floquet state.

It is well established¹⁻⁷ that a one dimensional (1D) Bose gas with a strong short range repulsion (or equivalently small density) - the Tonks-Girardeau gas, exhibits features of weakly interacting fermions. Can a similar phenomenon take place and be observed in dimensions larger than one? One example of statistical transmutation in 2D is provided by the composite boson picture of the fractional quantum Hall effect (FQHE)⁸⁻¹³. In this case the kinetic energy is totally degenerate due to the Landau quantization and the ground state is solely determined by the interactions. It was recently shown¹⁴⁻¹⁶ that it is actually enough to have the kinetic energy degenerate along a *line* in the 2D reciprocal space (so called “moat”) to achieve the statistical transmutation⁸. The moat-like dispersion was discussed earlier in context of Rashba spin-orbit coupling^{14,19-22}, and for certain lattices with more than one site per unit cell and next nearest neighbors hopping^{15,16,18}.

In this paper we show that the moat dispersion may be found even in simplest lattices (e.g. square) upon a suitable periodic driving. The lowest Bloch band adiabatically evolves into a Floquet band, which exhibits an approximately flat minimum along a closed contour encircling the Γ -point. Consequently the single particle density of states (DOS) diverges as inverse square root of energy at the bottom of the moat. Such 1D behavior of 2D DOS motivates the analogy with the Tonks-Girardeau case. The specific mechanism of the statistical transmutation in 2D, however, is very different from its 1D sibling. While the latter is achieved by simple sign inversion of the wave function at coinciding coordinates of particles, the former requires flux attachment, similar to FQHE.

As a result, the emerging 2D fermions are subject to the time reversal symmetry breaking effective magnetic field, and leading to a peculiar Landau spectrum. This state of bosons resembles the $U(1)$ level-1 version of chiral spin liquid^{16,23-25}, characterized by the topological order and the emerging of the statistical transmutation (fractionalized excitations typical for spin liquids²⁶⁻²⁸). The

chiral spin liquid was suggested by Kalmeyer and Laughlin in Ref. 23 as a possible ground state of frustrated spin systems. Here, instead of spin-1/2 operators, or alternatively hard-core bosons, one has interacting bosons forming a bosonic topological insulator. The latter is gapped in the bulk but supports gapless chiral excitations along edges. Below we show that both absence of condensation and the fermionic nature of the state may be detected through the velocity distribution of the released gas.

The Hamiltonian of interacting Bose gas with the moat dispersion relation can be written as

$$H = \frac{1}{2M} \sum_{\mathbf{r}} \left[\Phi_{\mathbf{r}}^{\dagger} \left(|\hat{\mathbf{k}} - k_0 \right)^2 \Phi_{\mathbf{r}} + 2g(\Phi_{\mathbf{r}}^{\dagger} \Phi_{\mathbf{r}})^2 \right], \quad (1)$$

where M is the mass of bosons, k_0 is the radius of the degenerate minima of the dispersion, g is the dimensionless contact interaction strength and $\Phi_{\mathbf{r}}^{\dagger}$, $\Phi_{\mathbf{r}}$ are corresponding boson creation and annihilation operators.

To engineer a system of spinless bosons effectively described by the Hamiltonian (1), we adopt the idea of Floquet optical lattice shaking developed in Ref. 29. The authors employed harmonically shifted 1D optical lattice at a near-resonance frequency corresponding to the lowest-band to the first-excited-band transition. As a result they have created a 1D dispersion relation with double minimum. The 2D generalization of this strategy is discussed below. A straightforward idea of using simple square lattice with the potential $\sim \sin^2(k_L x) + \sin^2(k_L y)$ does not work because of the separable (in x, y) nature of the potential. Indeed the corresponding bands are labeled by the two-integers ϵ_{n_x, n_y} with the lowest band being $\epsilon_{0,0}$. The low energy excited bands $\epsilon_{0,1}$ are $\epsilon_{1,0}$ are highly anisotropic and thus do not lead to a flat moat. The next excited band $\epsilon_{1,1}$ is approximately isotropic, but shaking the lattice either in x or y directions does not produce matrix elements between $\epsilon_{1,1}$ and $\epsilon_{0,0}$, due to orthogonality of the separable wave functions.

The simplest way to engineer an approximately flat moat is to create a square optical lattice with two sites

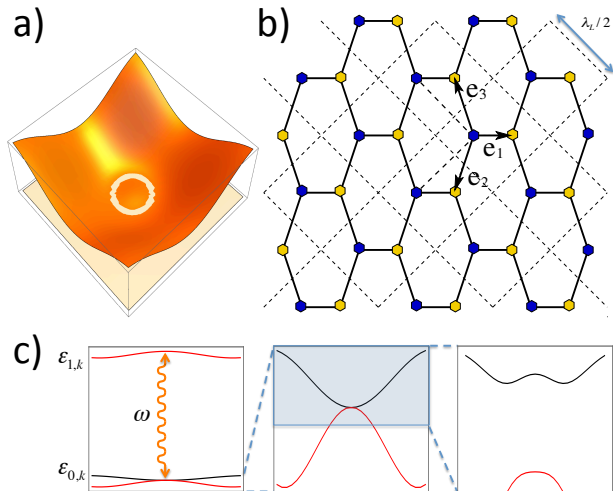


FIG. 1: (Color online) a) Lowest Floquet band exhibiting approximately flat moat. b) Fragment of a square optical lattice with two sites per unit cell³⁰ that gives rise to an approximately flat moat in the lowest Floquet band upon resonant driving. c) Left panel shows the band structure of the undriven optical lattice. The driving frequency ω is of order of the gap causing resonant coupling between the lowest and the first excited bands at $\mathbf{k} = 0$. Middle panel: enlargement of the lowest and shifted first excited bands. Right panel: Blow up of the driven lowest Floquet band exhibiting a double-well feature in $k_x + k_y$ direction indicating appearance of the moat in the Brillouin zone.

per unit cell. Such a lattice can be constructed by fusing a laser setup with laser beams of wavelength $\lambda_L = 2\pi/k_L$, resulting in a standing wave intensity pattern forming a regular square lattice, and then adding two additional identical laser beams directed along $x + y$ and $x - y$ diagonals (X scheme). If the lasers directed along x , y , and $x - y$ directions are calibrated to have exactly the same phases while the laser along $x + y$ diagonal has a phase shift amounting to π , such setup results in a potential

$$U(x, y) = U_0 \left[\sin^2(k_L x) + \sin^2(k_L y) + \sin^2[k_L(x - y)] + \cos^2[k_L(x + y)] \right]. \quad (2)$$

This potential realizes a square optical lattice of the depth U_0 , having two sites per unit cell (A and B), with vectors $k_L \mathbf{e}_1 = (\frac{\pi}{3}, \frac{\pi}{3})$, $k_L \mathbf{e}_2 = (\frac{\pi}{3}, -\frac{2\pi}{3})$ and $k_L \mathbf{e}_3 = (-\frac{2\pi}{3}, \frac{\pi}{3})$, depicted in Fig. 1. One can harmonically drive this lattice by applying time dependent phase shifts to the lasers, resulting into the transformation $x \rightarrow x - \Delta \cos \omega t$, $y \rightarrow y - \Delta \cos \omega t$, where Δ is the shaking amplitude. Below we show that, if the frequency ω is nearly resonant with two lowest bands, an almost flat moat appears in the lowest Floquet band.

The Lagrangian describing such a time-dependent

problem is given by

$$\mathcal{L} = \bar{\psi}(\mathbf{r}, t) \left\{ i\partial_t - \hat{H}(t) \right\} \psi(\mathbf{r}, t)$$

$$\hat{H}(t) = -\frac{\partial_{\mathbf{r}}^2}{2M} + U[x - x(t), y - y(t)], \quad (3)$$

where $\psi(\mathbf{r}, t)$ is a single particle wave function. Periodicity of lattice with $T_r = \pi/k_L$, implies that the solution $\psi_{n,\mathbf{k}}(\mathbf{r}, t)$ of the Schrödinger equation with Hamiltonian $\hat{H}(t)$, can be uniquely described by the space-time periodic single particle eigenstate $\varphi_{n,\mathbf{k}}(\mathbf{r}, t)$ of the Floquet operator $i\partial_t - H(t)$ as $\psi_{n,\mathbf{k}}(\mathbf{r}, t) = e^{iE_n(\mathbf{k})t} e^{i\mathbf{k}\mathbf{r}} \varphi_{n,\mathbf{k}}(\mathbf{r}, t)$. This representation is analogous to the Bloch representation of states in time independent periodic potentials. Here $E_n(\mathbf{k}) \in (0, \omega)$ is the Floquet energy of n 'th Bloch band, defined modulus of multiples of ω (corresponding to the energy quanta produced by driving). The Bloch momentum is given by $\mathbf{k} = 2\pi\mathbf{m}/L$, $\mathbf{m} = (m_x, m_y)$, $m_{x,y} = 1, \dots, L$, with L being the lattice size. Here the function $\varphi_{n,\mathbf{k}}(\mathbf{r}, t)$ is periodic in x and y directions with the period T_r , and in time with the period $T = 2\pi/\omega$. To find the Floquet spectrum we expand the periodic counterpart, $\varphi_{n,\mathbf{k}}(\mathbf{r}, t)$, of the Bloch eigenfunction in Fourier series over momenta $\frac{2\pi m_x}{T_r}$, $\frac{2\pi m_y}{T_r}$ and energies $\frac{2\pi s}{T}$ with integer $s, m_x, m_y \in (-\infty, \infty)$ and numerically diagonalize the Hamiltonian in this basis, assuming it is a large finite dimensional matrix. Diagonalization here yields the lowest quasienergy of the Floquet spectrum.

The distribution function of excitations in a periodically-driven system, generally speaking, can be obtained by solving a kinetic equation in the Floquet basis. However, in many relevant situations, an equilibrium-like distribution of quasi-steady states on Floquet bands has been shown to be the proper approximation^{31,32}. Furthermore, the results of the shaken-lattice experiment in one dimension²⁹, show that one can apply conventional statistical mechanics to Floquet systems of this sort (shaken lattices). The lowest quasienergy of the Floquet spectrum in this experiment appears to be the stationary, time independent kinetic energy of the system. This suggests that in our scheme one still arrives at a stationary, time independent problem of particles with kinetic energy given by the lowest Floquet band. Its shape, on the other hand, is affected by the closeness to the resonance with the help of the avoided crossings, and may acquire the moatlike form.

To understand the origin of the moat dispersion qualitatively consider the two lowest bands, $\epsilon_0(\mathbf{k})$ and $\epsilon_1(\mathbf{k})$, of the potential (3). Their Bloch functions $\varphi_{0,\mathbf{k}}(\mathbf{r})$ and $\varphi_{1,\mathbf{k}}(\mathbf{r})$ are correspondingly even and odd functions with respect to interchange of A and B sites of the unit cell, i.e. $x + y \rightarrow -x - y$. Figure 1c depicts these two bands for $U_0 = 11E_R$, where $E_R = k_L^2/2M$ is the recoil energy. The resonant shaking of the phases with frequency $\omega \approx \epsilon_1(0) - \epsilon_0(0) \approx 2.32E_R$ shifts the upper band as $\epsilon_1(\mathbf{k}) - \omega$ to touch the lower one at $\mathbf{k} = 0$ and induces the off diagonal matrix element $V_{\mathbf{k}}$ between these two

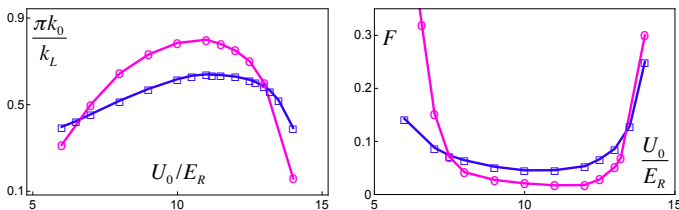


FIG. 2: (Color online) Left panel: characteristic radius k_0 plotted as a function of dimensionless U_0/E_R at two values of $k_L \Delta / \pi = 0.01$ (circles) and 0.02 (squares). Right panel: the flatness measure F of the moat versus U_0/E_R is shown. For definition see the main text.

bands. Due to the parity of the Bloch functions, the latter originates from the last term in Eq. (2) and is given by $V(\mathbf{k}) = \frac{U_0}{2} J_1(4k_L \Delta) \int d^2 \mathbf{r} \bar{\varphi}_{0,\mathbf{k}}(\mathbf{r}) \sin[2k_L(x+y)] \varphi_{1,\mathbf{k}}(\mathbf{r})$, where J_1 is the Bessel function. The effective two-band Hamiltonian

$$\mathcal{H}_{\mathbf{k}} = \begin{pmatrix} \epsilon_0(\mathbf{k}) & V(\mathbf{k}) \\ \bar{V}(\mathbf{k}) & \epsilon_1(\mathbf{k}) - \omega \end{pmatrix}. \quad (4)$$

yields the moat shape for the band, which is adiabatically connected to the original lowest Bloch band $\epsilon_0(\mathbf{k})$. Figure 2a shows dependence of the characteristic radius of the moat as a function of U_0 at two values of $k_L \Delta / \pi = 0.01$ and 0.02 . The moat appears at finite values of U_0/E_R and exists until about $U_0/E_R \lesssim 14$. Figure 2b shows the ratio of the difference of maximal and minimal energies along the moat, $E_{\max} - E_{\min}$, and the height of spectrum in the Γ point, $E_{\Gamma} - E_{\min}$, illustrating the flatness of the moat as function of U_0 .

An exactly flat Floquet moat band may be achieved by rotating of the lasers³³ in 1D optical lattices with the same resonant frequency as specified in Ref. [29].

Assuming an ideal moat, the interacting bosons are described by the Hamiltonian (1). Its single particle density of states diverges as $\epsilon^{-1/2}$, similar to the 1D case. This immediately suggests that the condensate can not be stable at any finite temperature. A more rigorous consideration, Ref. [34], starts from assuming a condensate in a state \mathbf{k}_0 along the moat and derives the anisotropic spectrum of Bogoliubov excitations $E_{\mathbf{p}} = [\epsilon_{\mathbf{p}}^2 + 2(gn/M)\epsilon_{\mathbf{p}}]^{1/2}$, where $\epsilon_{\mathbf{p}} = (|\mathbf{p} + \mathbf{k}_0| - k_0)^2 / 2M$. It is easy to see then that the fraction of thermally excited quasiparticles diverges as a power law (Ref. [34] deals with 3D, where divergence is only logarithmic) with the system size, indicating instability of the condensate at any finite temperature.

Moreover, there are compelling reasons to believe (see also Ref. 35) that the groundstate of the repulsively interacting bosons with the moat dispersion does not break $U(1)$ symmetry but breaks the time reversal symmetry. Thus the state is not represented by the condensate. It was argued in Refs. [14–16] that the better approximation to the actual ground state¹⁷ is the variational wave function, given by a Landau level fully filled

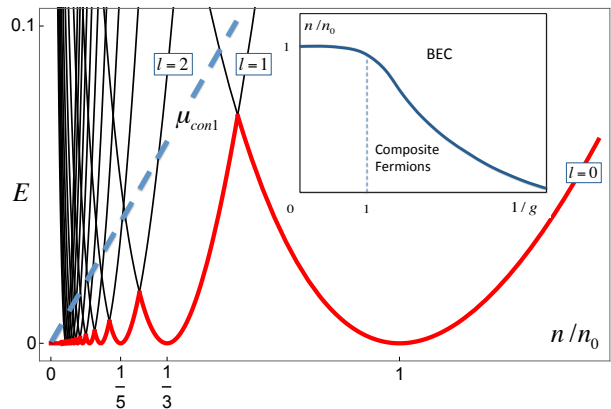


FIG. 3: (Color online) Excitation spectrum in units of E_R is plotted versus n/n_0 . The per particle energy, E_{gs}/E_R , represented by the fully filled lowest LL, is shown by the thick grey (red) curve. The thin black lines represent excited energies. Dashed line represents the chemical potential of a condensate μ_{con1}/E_R corresponding to the interaction parameter $g \sim 1$. The comparison between chemical potentials of these candidate states results in a phase diagram presented in the inset. For such strong interactions the transition from composite fermion state to zero temperature BEC takes place at densities $n/n_0 \sim 1$. Upon lowering g , the transition shifts towards smaller n/n_0 , as schematically shown in the inset.

with fermions, which are transformed to bosons with the Chern-Simons flux attachment (2D version of Jordan-Wigner fermionization^{36–38}):

$$\Phi(\mathbf{r}_1, \dots, \mathbf{r}_N) = e^{i \sum_{i < j} \arg[\mathbf{r}_i - \mathbf{r}_j]} \Psi_F(\mathbf{r}_1, \dots, \mathbf{r}_N). \quad (5)$$

Here $\Psi_F(\mathbf{r}_1, \dots, \mathbf{r}_N)$ is a fully antisymmetric state of N fermions. By this reason the wave function (5) does not cost *any* short-range interaction energy. The Chern-Simons phase $e^{i \arg[\mathbf{r}_i - \mathbf{r}_j]} = (z_i - z_j)/|z_i - z_j|$, with complex $z_j = x_j + iy_j$, is antisymmetric with respect to the exchange of any two coordinates, restoring the bosonic nature of $\Phi(\mathbf{r}_1, \dots, \mathbf{r}_N)$. The Chern-Simons factor costs kinetic energy, since it effectively modifies the momentum operator in Eq. (1) as $i\nabla_{\mathbf{r}} \rightarrow i\nabla_{\mathbf{r}} - \mathbf{A}(\mathbf{r})$, where the vector potential is given by

$$\mathbf{A}_{\alpha}(\mathbf{r}_i) = \varepsilon_{\alpha\beta} \sum_{j \neq i} \frac{(\mathbf{r}_i - \mathbf{r}_j)_{\beta}}{|\mathbf{r}_i - \mathbf{r}_j|^2}, \quad (6)$$

and $\varepsilon_{\alpha\beta}$ is an antisymmetric tensor. The Chern-Simons magnetic field, originating from \mathbf{A} is given by $B(\mathbf{r}_j) = \text{curl } \mathbf{A}(\mathbf{r}_j) = 2\pi \sum_{i \neq j} \delta(\mathbf{r}_i - \mathbf{r}_j) \equiv 2\pi n(\mathbf{r}_j)$, where $n(\mathbf{r})$ is the density operator.

By analogy with the fractional quantum Hall effect we first adopt a mean field approximation, which replaces a set of the flux lines with a *uniform* magnetic field $B(\mathbf{r}) \rightarrow B = 2\pi n$, where n is the average density. In this approximation Ψ_F is a state of non-interacting fermions with the dispersion relation $(|\mathbf{k}| - k_0)^2 / 2M$ placed in a uniform magnetic field B .

The energies of corresponding Landau levels are given by $E_l = (k_0^2/2M) \left[\sqrt{\frac{\omega_c}{(k_0^2/2M)}}(l+1/2) - 1 \right]^2$, where $\omega_c = B/M = 2\pi n/M$ and $l = 0, 1, 2, \dots$. The corresponding spectrum, shown in Fig. 3, consists of set of non-monotonic functions of the field (i.e. density), which reach zero energy at

$$n_l = \frac{k_0^2}{4\pi(l+1/2)}. \quad (7)$$

At this particular set of densities the fermionic wave function is given by the fully occupied (indeed there is exactly one flux quanta per particle) l -th Landau level:

$$\Psi_F^{(l)}(\mathbf{r}_1, \dots, \mathbf{r}_N) = \frac{1}{\sqrt{N!}} \det_{m,j} \left[\chi_m^{(l)}(\mathbf{r}_j) \right], \quad (8)$$

where $\chi_m^{(l)}(\mathbf{r}) = (2\pi(l+m)!!)^{-1/2} (b^\dagger)^{l+m} (a^\dagger)^l [e^{-\frac{1}{4}|z|^2}]$, is a state with the angular momentum $m = -l \dots -l + N$ at the Landau level l . Here $a^\dagger = \frac{1}{\sqrt{2}}(\frac{z}{2} - 2\frac{\partial}{\partial z})$, $b^\dagger = \frac{1}{\sqrt{2}}(\frac{z}{2} - 2\frac{\partial}{\partial \bar{z}})$ are the ladder operators. For intermediate densities $n_{l+1} < n < n_l$ the ground state is a mixture of two fermion liquids with densities n_l and n_{l+1} . The variational state (5), (8) breaks time-reversal symmetry due to the effective Chern-Simons magnetic field, however it conserves the $U(1)$. Though within the mean-field approximation the state has zero energy, its actual energy is given by the expectation value of the Hamiltonian operator (1) (or rather only its kinetic energy part). The corresponding calculations, given in the supplementary material,³⁹ show that the energy per particle scales as $E(n) \sim \frac{k_0^2}{M} \left(\frac{n}{n_0}\right)^2 \log^2(n/n_0)$. This should be compared with either the naive estimate for the condensate state $E \sim gn/M$, or the result of Ref. [35] $E \sim n^{4/3}$. In any event, the composite fermion variational state (5), (8) is seen to be parametrically advantageous at small enough density.⁴² The comparison of chemical potentials of candidate BEC states and of our composite fermion state resulted in a phase diagram presented in Fig. 3(inset).

The composite fermion state discussed above represents an example of a topological state of bosons. To achieve this state experimentally, one needs to load the driven lattice of Fig. 1 with bosons and let them occupy the degenerate lowest steady Floquet band. An important and somewhat indirect experimental measure of the composite fermion state of bosons is the velocity distribution of an expanding gas, which can be observed in the time of flight experiments⁴³.

The group velocity of an expanding gas is defined by the derivative of the kinetic energy as $\mathbf{v} = \partial_{\mathbf{k}} \frac{(|\mathbf{k}| - k_0)^2}{2M} = \frac{|\mathbf{k}| - k_0}{M} \frac{\mathbf{k}}{|\mathbf{k}|}$. Expectation value of this operator in the proposed state of composite fermions (5), (8) is obtained numerically and depicted in Fig. 4. The result demonstrates striking difference with the velocity distribution of condensed bosons shown in the inset of Fig. 4. While at high temperatures distribution functions of condensate

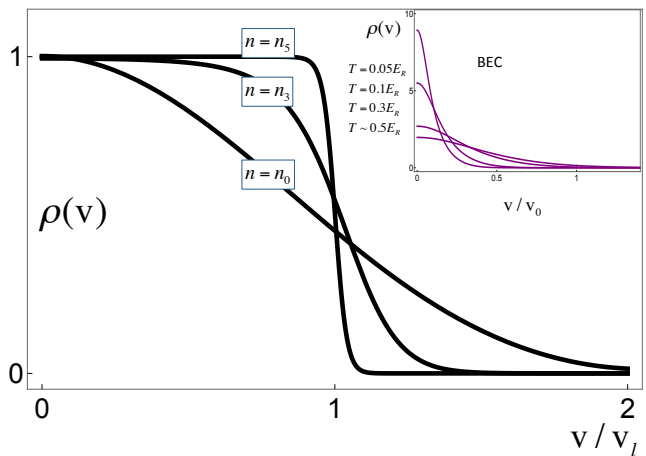


FIG. 4: (Color online) Dimensionless velocity distribution $\rho(v) \cdot v_l$, where $mv_l = \pi n_l/k_0$, of an expanding gas of composite fermions plotted vs dimensionless velocity v/v_l at fixed values of density $n = n_l$, $l = 0, 3, 5$ and zero temperature. Inset: Dimensionless velocity distribution of condensed bosons with density $n = n_0$. The temperatures are marked. At low temperatures the distribution shows a sharp peak at zero velocity, which is absent in the distribution of the composite fermions.

and of composite fermion state are similar, the qualitative difference at $T \rightarrow 0$ is caused by the fermionic nature of the latter. If for condensed bosons the distribution is sharply peaked at $v = 0$, indicating condensation into a state with zero velocity, for composite fermions it is reminiscent to the Fermi-Dirac distribution exhibiting weak, plateau-like behavior at finite v at very low temperatures and small densities. Importantly, at low temperatures, there is no sharp peak at $v = 0$. The plateau vs peak difference can be regarded as the indication of the proposed statistical transmutation. In the field-theoretical language this difference can be traced back to the presence of the effective Chern-Simons magnetic field and to the fact that effectively fermions find themselves in a state corresponding to the fully occupied lowest Landau level. Unambiguous experimental identification of the composite fermion state may require additional probes, such as measuring collective modes spectrum, which is sensitive to the equation of state.

To conclude, we note that the ability to control and probe statistical transmutation in quantum many body systems is one of the most fundamental challenges in contemporary physics. In this letter we propose an experimental scheme to (i) engineer a resonantly driven bosonic system exhibiting a moat-band and the phenomenon of transmutation of statistics, and (ii) probe our prediction for the velocity distribution in time of flight experiments at low densities. The proposed state for bosons in a moat band is energetically more efficient at low densities than any other known candidate for the ground state. It realizes a Floquet topological phase of bosons, joining the family of other topological structures

achieved in non-equilibrium including the Floquet topological insulators⁴⁴⁻⁴⁶ and superfluids⁴⁷.

This work was supported by the PFC-JQI (T.S.), US-

ARO, Australian Research Council, and Simons Foundation (V.G.), and DOE contract DE-FG02-08ER46482 (A.K.).

-
- ¹ L. Tonks, Phys. Rev. 50, 955 (1936).
² M. Girardeau, J. Math. Phys. 1, 516 (1960).
³ E. H. Lieb and W. Liniger, Phys. Rev. 130, 1605 (1963).
⁴ C. N. Yang, Phys. Rev. Lett. 19, 1312 (1967).
⁵ M. Gaudin, Phys. Lett. A 24, 55 (1967).
⁶ B. Paredes, A. Widera, V. Murg, O. Mandel, S. Fölling, I. Cirac, G. V. Shlyapnikov, T. W. Hänsch, and I. Bloch, Nature (London) **429**, 277 (2004).
⁷ T. Kinoshita, T. Wenger, and D. S. Weiss, Science **305**, 1125 (2004).
⁸ A. M. Polyakov, Mod. Phys. Lett. A **3**, 325 (1988).
⁹ J. K. Jain, Phys. Rev. Lett. **63**, 199 (1989).
¹⁰ A. Lopez and E. Fradkin, Phys. Rev. B **44**, 5246 (1991).
¹¹ B. I. Halperin, P. A. Lee, and N. Read, Phys. Rev. B **47**, 7312 (1993).
¹² R. Shankar, Ann. Phys. (Berlin) **523**, 751 (2011).
¹³ T. S. Jackson, N. Read, and S. H. Simon, Phys. Rev. B **88**, 075313 (2013).
¹⁴ T. A. Sedrakyan, A. Kamenev, and L. I. Glazman, Phys. Rev. A **86**, 063639 (2012).
¹⁵ T. A. Sedrakyan, L. I. Glazman, and A. Kamenev, Phys. Rev. B **89**, 201112(R) (2014).
¹⁶ T. A. Sedrakyan, L. I. Glazman, and A. Kamenev, Phys. Rev. Lett. **114**, 037203 (2015).
¹⁷ Numerical comparison between the ground state energies at higher densities, corresponding to the half-filled optical lattice, obtained by our method, with the available result of exact diagonalization¹⁸, yields a small 3-5 % difference. This adds confidence that our state is a good starting point and is quite close to the true groundstate.
¹⁸ C. N. Varney, K. Sun, V. Galitski, and M. Rigol, Phys. Rev. Lett. **107**, 077201 (2011).
¹⁹ Y. A. Bychkov and E. I. Rashba, J. Phys. C **17**, 6039 (1984).
²⁰ V. Galitski and I. B. Spielman, Nature (London) **494**, 49 (2013).
²¹ D. L. Campbell, G. Juzeliūnas, and I. B. Spielman, Phys. Rev. A **84**, 025602 (2011).
²² E. Berg, M. S. Rudner, and S. A. Kivelson, Phys. Rev. B **85**, 035116 (2012).
²³ V. Kalmeyer and R. B. Laughlin, Phys. Rev. Lett. **59**, 2095 (1987).
²⁴ X. G. Wen, F. Wilczek, and A. Zee, Phys. Rev. B **39**, 11413 (1989).
²⁵ S.-S. Gong, W. Zhu, and D. N. Sheng, Sci. Rep. **4**, 6317 (2014); B. Bauer, L. Cincio, B. P. Keller, M. Dolfi, G. Vidal, S. Trebst, and A. W. W. Ludwig, Nat. Commun. **5**, 5137 (2014).
²⁶ A. Kitaev, Annals of Physics **321**, 2 (2006).
²⁷ L. Balents, Nature **464**, 199 (2010).
²⁸ C. A. Lamas, A. Ralko, D. C. Cabra, D. Poilblanc, and P. Pujol, Phys. Rev. Lett. **109**, 016403 (2012); B. Normand and Z. Nussinov, arxiv:1503.0727.
²⁹ C. V. Parker, L.-C. Ha, and C. Chin, Nature Phys. **9**, 769 (2013).
³⁰ The optical lattice under consideration is different from the tunable honeycomb optical lattice realized in L. Tarruell, D. Greif, T. Uehlinger, G. Jotzu, and T. Esslinger, Nature **483**, 302 (2012); G. Jotzu, M. Messer, R. Desbuquois, M. Lebrat, T. Uehlinger, D. Greif, and T. Esslinger, Nature **515**, 237 (2014).
³¹ V. M. Galitskii, S. P. Goreslavskii, and V. F. Elesin, Sov. Phys. JETP **30**, 117 (1970).
³² K. I. Seetharam, C.-E. Bardyn, N. H. Lindner, M. S. Rudner, and Gil Refael, preprint arXiv:1502.02664.
³³ J. Radić, T. A. Sedrakyan, I. B. Spielman, and V. Galitski Phys. Rev. A **84**, 063604 (2011).
³⁴ S. A. Brazovskii, Sov. Phys. JETP **41**, 85 (1975).
³⁵ S. Gopalakrishnan, A. Lamacraft, and P. M. Goldbart, Phys. Rev. A **84**, 061604(R) (2011).
³⁶ J. Ambjorn and G. Semenoff, Phys. Lett. B **226**, 107 (1989).
³⁷ E. Fradkin, Phys. Rev. Lett. **63**, 322 (1989).
³⁸ Y. R. Wang, Phys. Rev. B **43**, 3786 (1991); Y. R. Wang, Phys. Rev. B **43**, 13774 (1991); Y. R. Wang, Phys. Rev. B **46**, 151 (1992).
³⁹ See Supplemental Material [url], which includes Refs. 40, 41.
⁴⁰ L. D. Landau and L. M. Lifshitz, "Quantum Mechanics, Third Edition: Non-Relativistic Theory", Elsevier Science Ltd. 2003.
⁴¹ I. L. Aleiner and L. I. Glazman, Phys. Rev. B **52**, 11296 (1995).
⁴² A word of caution here is in order. The thermodynamic limit $N \rightarrow \infty$ reaches slowly suggesting strong finite size corrections to the fluctuation effects. The finite size corrections scale with density linearly as argued in the Supplementary material and shown numerically using Monte-Carlo simulations in J. Radić and V. Galitski (unpublished).
⁴³ I. Bloch, J. Dalibard, and W. Zwerger, Rev. Mod. Phys. **80**, 885 (2008).
⁴⁴ N. H. Lindner, G. Refael, and V. Galitski, Nature Physics **7**, 490 (2011).
⁴⁵ Y. T. Katan and D. Podolsky, Phys. Rev. Lett. **110**, 016802 (2013).
⁴⁶ P. Titum, N. H. Lindner, M. C. Rechtsman, and G. Refael, Phys. Rev. Lett. **114**, 056801 (2015).
⁴⁷ M. S. Foster, V. Gurarie, M. Dzero, and E. A. Yuzbashyan, Phys. Rev. Lett. **113**, 076403 (2014).